Determination of the magnetic surfaces in the stellarator W Ib by the use of a pulsed electron beam

E.Berkl
G.v.Gierke
G.Grieger

IPP 2/69 Juni 1968

INSTITUT FÜR PLASMAPHYSIK
GARCHING BEI MÜNCHEN

INSTITUT FÜR PLASMAPHYSIK

GARCHING BEI MÜNCHEN

Determination of the magnetic surfaces in the stellarator W Ib by the use of a pulsed electron beam

E.Berkl

G.v.Gierke

G.Grieger

IPP 2/69 Juni 1968

Die nachstehende Arbeit wurde im Rahmen des Vertrages zwischen dem Institut für Plasmaphysik GmbH und der Europäischen Atomgemeinschaft über die Zusammenarbeit auf dem Gebiete der Plasmaphysik durchgeführt.

IPP 2/69 E.Berkl
G.v.Gierke
G.Grieger

Determination of the magnetic surfaces in the stellarator W Ib by the use of a pulsed electron beam.

June 1968 (in English)

Abstract

By means of a pulsed electron beam the properties of the magnetic field of the stellarator W Ib were investigated, e.g. existence and shape of magnetic surfaces, rotational transform, shear. The existence of magnetic surfaces can be considered as proved with a certainty of 700 : 1. The experimental value of the rotational transform is 12 % less than the calculated one, the shear is of interesting magnitude.

The existence and the shape of the magnetic surfaces as well as the magnitude of the rotational transform are of extreme importance for the behaviour of plasma in a stellarator magnetic field, and the knowledge of these properties is necessary for the interpretation of experimental results.
In earlier investigations of that kind an electron beam has been used to excite the atoms of the residual gas so that the emitted light gave a picture of the path of the beam. This method yielded only rough information on the angle of the rotational transform and the shape of the magnetic surfaces.
In connection with the results obtained on plasma confinement in the stellarator W Ib [1] three main questions arose:
1. To which extend do magnetic surfaces exist in W Ib;
2. what are the exact values of the rotational transform; and
3. is there any shear in the magnetic field?

Therefore, a more refined experiment has been made where the drift surfaces of a pulsed electron beam have been studied.

Experimental arrangement

1. The stellarator W Ib (see fig. 1) has the shape of a race track. The radius of curvature of the U-bends is R = 35 cm, the length of the straight sections 49.6 cm, yielding a total length of the machine of L = 319 cm. The diameter of the vacuum tube is $2r_V$ = 5.0 cm. During the plasma experiments mentioned above a limiter was inserted into one of the straight sections which determined the aperture by its circular opening of $2r_A$ = 3.0 cm diameter.

   The main magnetic field is excited by 114 equally spaced coils, each of them 1.4 cm thick and with a bore of 9.2 cm in diameter. The helical windings are of the type l = 2 and form a right hand screw with 1.7 revolutions per U-bend. The helical current is carried by a bundle of 8 wires which fill an angle of 52.2

degrees (measured from the axis of the vacuum tube) and have a radial extension from 3.75 to 4.15 cm (see fig. 2). At the ends of each U-bend circularizers are added which are formed by a halved pitch of the helical wires over half a period of the helical field. These circularizers are supposed to deform the elliptical cross sections of the magnetic surfaces into circular ones if one passes from a U-bend to a straight section. According to [2] the following connection between the angle of the rotational transform, ι, and the currents, J_H and J_z, generating the helical field and the main field respectively is expected to be

$$\iota = 0.63\pi \cdot \left(\frac{J_H}{J_z}\right)^2 \qquad (1)$$

It should be kept in mind, however, that equation (1) is only an approximate relation obtained for an idealized picture, where, particularly, the effect of curvature has been neglected. According to eq.(1) ι is constant over the cross section.

If no limiter is inserted into the machine the aperture is determined by the magnetic surface which is just touching the wall of the vacuum vessel. This will happen especially in the U-bend where the ellipticity of the magnetic surfaces is large. The size of the aperture is the cross section of the magnetic surface as defined above. The magnetic field was d-c operated. The strength of the main magnetic field was 2 kГ. During the course of the experiments it turned out that the current fluctuations of the generators, as small as they were, disturbed the accuracy of the results since they entered quadratically in the rotational transform. In order to avoid this influence the helical windings have been connected in series with the coils of the main magnetic field so that only one generator had to be used. In this case the rotational transform could not be varied continuously but only step by step. This was done by disconnecting a certain number of the wires forming the helical windings. Unfortunately, this procedure also yields a change in the distribution of the helical currents as can be seen from fig. 2. On the other hand, this behaviour

might provide a possibility to change the shear of the magnetic lines independent of the value of the rotational transform as will be shown later.

Two pairs of correction coils are installed, their plane being parallel to the plane of the torus. These coils allow the excitation of small magnetic fields being perpendicular on the magnetic axis and having an angle of $\pm$ 45° with respect to the plane of the torus. This angle and the magnitude of this correction field can be changed to any desired value by a suitable superposition of these two fields which then lead to a displacement of the magnetic axis perpendicular to the direction of the applied field. The magnitude of this displacement, Δr, for the stellarator W Ib is given by the relation

$$\Delta r = - 101 \frac{B}{B_z} \cdot \frac{\Pi}{\iota} \text{ cm} \qquad (2)$$

where

$$B = 4.4 \frac{\Gamma}{100A} \qquad (3)$$

2. The electron beam is generated by a tiny gun, the anode of which was a tube of 2 mm outer diameter made of stainless steel and closed at the top. It was electrically connected with the wall of the vacuum vessel and with ground. The wall of this tube was provided with a hole of 0.5 mm diameter and an oxid coated cathode placed immediately behind it. Typical beam currents of 0.3 mA have been achieved when the cathode was put on - 115 V with respect to ground. A voltage of 115 V has been chosen as acceleration voltage as a compromise between a sufficiently low v and sufficiently large beam current. In addition, the time of flight around the machine is just 0.5 µsec for 115 V-electrons.

   The first experimental results have shown that the single particle drift surfaces , if measured by a continuously running electron beam, were badly disturbed by space charge effects. These effects were greatly reduced when the cathode voltage

was pulsed so that only one bunch of electrons at a time was running around the machine. This method - which has been used throughout all experiments mentioned from now on - provided the additional advantage of easily determining the time of flight and thus the number of revolutions covered by the beam at the time when it is collected by the probe.

For the pulsed operation of the electron gun a 50 Ω-resistor was connected parallel to the gun and a cable was discharged across it by means of a Hg-relay. The square wave pulse thus obtained had a duration of 1 μsec and was flat within a few percent. The rise time was about 20 nsec, the repetition rate 50/sec.

The electron gun was arranged at one of the straight sections and could be put at any desired position of the cross section of the vacuum tube. But preferably such positions have been chosen for which the support of the gun had a minimum interference with the drift surface under investigation. By twisting the gun about its axis cathode and hole in the anode could be aligned with respect to the magnetic lines, in which case the beam current was maximum. On the opposite side of the machine two probes were introduced into the vacuum tube, one from the top and one from the bottom. The sensitive parts of the probes were discs of .5 mm in diameter.For minimum disturbance of the drift surfaces by electrostatic effects at all probe positions the probe shafts had been hooked by an angle of 45° at a distance of 5 mm from the tip. Furthermore, the probe shafts had been provided with metallic shields of 1 mm outer diameter which had been put to ground potential. A voltage of +20 V was applied to the probe in order to prevent the emission of secondary electrons. It has been checked that this voltage did not affect the position of the electron beam when the probe was placed for maximum probe current. These precautions yielded reliable results down to drift surfaces of 14 mm diameter. Smaller drift surfaces were still disturbed and had to be excluded from examination.

The probes could be moved across the cross section of the tube

and placed in any position with an accuracy of ± 1 mm. The probe current has been measured by means of an oscilloscope which was triggered by the gun pulse. When the probe was adjusted to maximum probe current, the position of the beam and the number of its revolutions (from the time delay between the gun pulse and the appearance of the peak) was obtained simultaneously. The time-of-flight measurement, however, allowed the determination of the number of revolutions only within ± 5 % because of the spread of the parallel velocity of the electrons. For longer times the beam becomes broader in time but was still relatively sharp in space. Therefore arguments of conservation of magnetic flux yield an accurate indication also for higher numbers of revolutions than 10.

Measurements

The first measurement was concerned with the accuracy of the main (toroidal) magnetic field. It was found that there was a misalignment of the electron beam in excess of the usual torus-drift of the electrons and therefore a misalignment of the magnetic lines. Upon applying a suitably chosen correction field the magnetic lines could be made to close upon themselves. However, as the correction field necessary for alignment had an angle of nearly 45° with respect to the plane of the torus it was found to be much more convenient to compensate only the main part of the field disturbance and allow for a small rest of misalignment. This way only one pair of the correction loops was necessary to be energized and the influence of current fluctuations could be minimized. In fig. 3 the dotted line indicates the current supplied to the correction coils and the residual displacement of the magnetic lines in radial direction, ΔR, and vertical (perpendicular to the plane of the torus) direction, Δh. This residual displacement of the field lines should result only in a small displacement, Δx, of the magnetic axis when the helical fields are applied. The magntiude of this

displacement can be obtained from eq.(2).
Five points were of particular interest to be investigated:

1) The existence of magnetic surfaces;
2) The shape of the magnetic surfaces;
3) The magnitude of the rotational transform;
4) The magnitude of the shear of the magnetic field;
5) The size of the aperture.

As for 1), the existence of magnetic surfaces - or more correctly, of drift surfaces - in this apparatus seems to be guaranteed within the accuracy of this experiment by the following observations:

a) In all cases if electrostatic disturbances could be avoided, electrons could be detected only on a particular "surface" - the correspondent drift surface - with an annular cross section having a radial extension of the magnitude δ. δ was only slightly larger than the sum of beam and probe diameter+). Inside as well as outside the hollow cylinder as defined above no electrons could be detected.

b) If the rotational transform ι, i.e. $\iota/2\pi$, is rational

$$\iota = \frac{m}{n}$$

with m, n as not too large integers, then the electron beam penetrates the cross section under observation at the identical point always after n revolutions around the machine provided the fraction $\frac{m}{n}$ is irreducible. Furthermore, if the position of the probe is chosen such that it picks up only a fraction of the electrons passing by, then a sequence of peaks

---

+) It is believed that the electric field around both the probe and the gun is responsible for the slight increase of δ above the geometrical value. This is supported by the observation that δ is increasing with increasing potential applied to the probe.

can be observed on the oscilloscope having a time spacing of $n \cdot \tau$, where τ is the time necessary for one revolution (see fig. 4). Naturally, the amplitude of the peaks is decreasing from peak to peak due to the electrons lost on the probe and the gun. By this argument it is clear that only a limited number of peaks could be observed. It is also clear that the total number of revolutions corresponding to the individual peaks is largest for largest time interval between the peaks which is the case for n being large. Therefore, for small values of n about 100 revolutions around the machine could be observed, but up to 700 for large n values. No particular attempt has been made to increase this number.

As point 2) is concerned, fig. 5 shows a number of nested drift surfaces. In this case it was the intention to investigate the "fine structure" of the magnetic surfaces. Therefore, a large number of beam positions has been measured in order to obtain a sufficiently "dense population" of the drift surfaces, and no particular knowledge of the corresponding time of flight is necessary to answer this question. The accuracy and reproducibility of all the individual probe positions at which the electron beam can be detected are about $\pm$ 2 mm. Therefore, one would be lead to the conclusion that the fine structure of these drift surfaces is of the particular form shown in fig. 5. On the other hand, it has been found that the probe itself has some effect on the path of the electron beam. This expresses itself particularly in a hysteresis (sticking) of the current collected by the probe when moving the probe across the drift surface. The position of the beam is also slightly displaced if the probe shaft is tangent to the drift surface. This is illustrated by the mutual distance of a number of groups of points having the same index. These points have been measured by two different probes introduced from the top and the bottom of the machine respectively and which have been carefully adjusted with respect to each other.

From these points of view it cannot be concluded whether the

apparent deviations from a smooth magnetic surface have any significance, but it is believed that the drift surfaces are much more regular than they appear to be. The intersections of the drift surfaces with a plane being perpendicular on the tube axis - these are the curves plotted - were expected to have a nearly circular shape. This is so since the probes have been arranged in the straight sections of the machine and the ends of the U-bends were provided with circularizers. The curves found, however, have clearly a more or less elliptic shape indicating that the circularizers are not working properly. In addition, the ellipticity found is much larger in the northern part of the machine (figs. 5 - 15) than it is in the southern one (figs. 16 - 20). The only difference in these two measurements was that in the northern part of the machine the probe was placed in equal distance from both U-bends whereas in the southern part of the machine it was positioned rather near (about 6 cm) to one of the circularizers, which, however, should not explain the difference in the results. It should be noted at this point that the current feeds to the helical windings were arranged on the northern side of the machine and their stray fields might have some influence on the shape of the magnetic surfaces. In order to obtain information on the magnetic surfaces from the measured drift surfaces data have been taken for both directions of the electron beam, parallel and antiparallel to the direction of the magnetic field, and the electron gun has been positioned in that manner that corresponding drift surfaces intersect each other at a common penetration point of the beam. This point defines the magnetic surface under observation, which should be "the mean" of the corresponding drift surfaces. Curves thus obtained are shown in figs. 6 - 20. (In cases in which only one curve is shown, the other could not be measured as the beam hit the gun already after a few revolutions around the machine.)

3. The angle of the rotational transform was measured from the angular displacement of the individual penetration points through the plane of reference (probe plane). The different points have been numbered according to the number of revolutions covered by the beam before reaching the probe. It can clearly be seen from the figures that the angular displacement from one penetration point to the next is not constant along the curve but is relatively small where the separation between two neighboured drift surfaces is large and vice versa. This behaviour is in agreement with arguments of conservation of magnetic flux.
Since ι is defined as the mean value of the rotational transform for the magnetic surface under consideration it has been evaluated in the following form: Assume $n \cdot \iota \approx 2k\Pi$, where n and k are integers, then ι was obtained by

$$\iota = \frac{1}{n(N+1)} \sum_{\nu=0}^{N} (\varphi_{n+\nu} - \varphi_{\nu}) \qquad (3)$$

φ_{ν} being the angular displacement between the first and the $(\nu + 1)^{th}$ penetration point. The values of k used were 1, 2, or 3. The values of ι thus obtained vs. the mean radius, r, of the drift surfaces have been plotted in fig. 21, where r is the geometric mean between the two axes of the ellipses. The curves for smaller values of ι - the lower curves of fig. 21 - have been found by disconnecting a certain number of wires forming the helical windings, as already mentioned. For the particular distributions of the helical currents which have been investigated see fig. 21.
At first it was thought that the method of measuring sequences, as explained above, would provide a mean to determine ι very accurately. However, it turned out that in this case the beam experienced an additional displacement every time it passed by the probe. This deviation would accumulate so that the error could easily become unallowable large. Therefore, this method had to be disregarded for the final results.

4. In order to give information on the shear of the magnetic field, ι is expanded into a potential series of ς, ς being a normalized radius

$$\iota = \sum_{\nu=0}^{\geq} \iota_\nu \varsigma^\nu \tag{4}$$

If one defines a case with $\iota \equiv \iota_o$ as to have no shear then the quantity

$$\frac{\partial \theta}{\partial r} = \frac{1}{L} \sum_{\nu=1}^{\geq} (\nu + 1)\iota_\nu \varsigma^\nu \tag{5}$$

gives the shear of the magnetic lines, L being the length of the machine. The reciprocal of this expression is knwon as the shear length L_s

$$L_s = \frac{L}{\sum_{\nu=1}^{\geq} (\nu + 1)\iota_\nu \varsigma^\nu} \tag{6}$$

For the three cases investigated the following numbers have been obtained from fig. 21

$$\begin{aligned}
&\text{case A:} \quad \iota_o = 0.500\ \Pi \quad \iota_1 = 0.034\ \Pi \quad \iota_{\nu>1} = 0 \\
&\text{case B:} \quad \iota_o = 0.278\ \Pi \quad \iota_1 = 0.026\ \Pi \quad \iota_{\nu>1} = 0 \\
&\text{case C:} \quad \iota_o = 0.130\ \Pi \quad \iota_1 = 0.030\ \Pi \quad \iota_{\nu>1} = 0
\end{aligned} \tag{7}$$

So the mean shear length turns out to be 18 m.
For the evaluation of earlier experiments with plasma in W Ib ι has been calculated under a number of simplifying assumptions but taking into account the effect of the circularizers. For the conditions of case A the calculated value of ι was

$$\iota_{calc} = 0.63\ \Pi \tag{8}$$

and nothing was known about its ς-dependence.
A comparison with the values given in (7) shows that the measured value of ι is only slightly smaller than ι_{calc} at the wall of the vacuum vessel ($\varsigma = 2.5$) but it is considerably smaller in the neighbourhood of $\varsigma = 0$ which is the region usually filled with plasma. At the axis one finds

$$\left(\frac{\iota_{exp}}{\iota_{calc}}\right)_o = 0.81 \qquad (9)$$

Theoretically, ι should be proportional to the square of the current flowing in the helical windings if keeping all other parameters constant. Relating ι_o of cases B and C to the one of case A one would expect according to this law

$$\text{case B: } \iota_{o\ expected} = 0.218\ \Pi \qquad \iota_{1\ expected} = 0.015\ \Pi \qquad (10)$$
$$\text{case C: } \iota_{o\ expected} = 0.160\ \Pi \qquad \iota_{1\ expected} = 0.011\ \Pi$$

These curves are indicated by dotted lines in fig. 21. It is concluded that their deviation from the experimental curves is caused by the simultaneous change of the current distribution when changing the magnitude of the helical current. At this point it is interesting to note that ι_1 is practically constant for all the three cases investigated. This behaviour offers the possibility of changing the rotational transform independently of the shear of the magnetic lines.

5. The aperture valid for experiments with plasma in W Ib can be found by selecting the largest magnetic surface not yet touching the limiter (particle detector) used in these experiments.

Comparison between measured and calculated drift surfaces

For comparison the drift surfaces and the individual penetration points of the electron beam through a plane of reference have also been calculated numerically+). This has been done under the simplifying assumption that the magnetic surfaces have circular cross sections in the straight section of the device. Magnitude of rotational transform and shear have been adopted from the experimental results.

For this calculation the path of the beam is projected into a plane of reference (plane of the probe) being perpendicular on the tube axis. In this description the beam carries out an angular motion with the angular velocity $\vec{\omega}_r$. In the same way the vector $\vec{\iota}$ describes its angular displacement if the beam passes once around the machine. Both $\vec{\omega}_r$ and $\vec{\iota}$ are perpendicular on the plane of reference. Under these circumstances the projected motion of the electron beam obeys the following relation (as long as curvature effects are neglected)

$$\vec{\omega}_r \times \vec{r} = \frac{v_{\parallel}}{L} (\vec{\iota} \times \vec{r}) \qquad (11)$$

$$= \frac{v_{\parallel}}{L} \sum_{\nu \geq 0} \varsigma^{\nu} (\vec{\iota}_{\nu} \times \vec{r}) \qquad (12)$$

where $v_{\parallel}$ is the parallel velocity of the electrons, L the length of the machine and $\vec{\iota}$ has been replaced by eq.(4). In order to obtain a more accurate picture two drift motions have to be superimposed upon eq.(12).There is at first the curvature drift, the essential contribution of which being caused by the curvature of the main magnetic field, $\frac{1}{R} = k$ alone which is for electrons

---

+) We thank Dr. R. Gorenflo and Miss Ch. Raschewa who have performed the numerical calculations.

$$\vec{v}_{D1} = \frac{m\, v_{\parallel}^2}{e\, B^2}\, \vec{B} \times \vec{K} \qquad (13)$$

Contributions arising from the helical motion of the beam shall be neglected. For the parameters used in this experiment

$$v_{D1} = 3.33 \cdot 10^5 \frac{cm}{sec} \qquad (14)$$

As has been mentioned already there was also a residual misalignment of the magnetic lines of the"toroidal" magnetic field.This can be accounted for by an additional unidirectional drift motion with a velocity, v_{D2}

$$v_{D2} = 1.4 \cdot 10^5 \frac{cm}{sec} \qquad (15)$$

The direction of this drift velocity is given by the displacement vector of the magnetic lines, the quantity of which can be obtained from fig. 3 .
The motion of the beam within the plane of reference is then obtained by a superposition of the individual contributions

$$\vec{v}_{\pm} = \pm\, \vec{\omega}_r x\, r + \vec{v}_{D1} \pm \vec{v}_{D2} \qquad (16)$$

where + or - stands for the two different directions of the beam, parallel or antiparallel to $\vec{B}$. Upon introducing cylindrical coordinates and integrating eq.(16) one obtains the equation of the trajectories (cross section of the drift surfaces) in implicite form

$$(v_{D1} \pm v_{D2}\cos\varphi_2)\cos\varphi \pm v_{D2}\sin\varphi_2 \sin\varphi = \frac{C}{\varrho} \pm \frac{v_{\parallel} r_w}{L} \sum_{\nu=0}^{\geq} \frac{\iota_\nu}{\nu+2}\, \varrho^{\nu+1} \qquad (17)$$

r_w being defined by $r = \varrho \cdot r_w$, C being the group parameter.
Drift surfaces have been measured for the two directions of the electron beam. If ϱ_o, φ_o is the point where the two curves belonging to one another intersect each other, then the corresponding group parameters $C_{o\pm}$ are defined by

$$C_{o\pm} = \varsigma_o[(v_{D1} \pm v_{D2}\cos\varphi_2)\cos\varphi_o \pm v_{D2}\sin\varphi_2\sin\varphi_o] \pm \frac{v_{//}\, r_w}{L} \sum_{\nu=0}^{\geq} \frac{\iota_\nu}{\nu+2}\varsigma_o^{\nu+2} \qquad (18)$$

With the help of eq.(17), eq.(16) can be split up into two differential equations.

$$\varphi = \frac{C}{\varsigma^2 r_w} \pm \frac{v_{//}}{L} \sum_{\nu=0}^{\geq} \frac{\nu+1}{\nu+2}\iota_\nu \varsigma^\nu \qquad (19)$$

$$\dot{\varsigma} = \frac{1}{r_w}[(v_{D1} \pm v_{D2}\cos\varphi_2)\sin\varphi \mp v_{D2}\sin\varphi_2\cos\varphi] \qquad (20)$$

Eqs. (19) and (20) have been integrated numerically starting from the point of intersection ς_o, φ_o, which has been taken from the experimental result. This way the cross section of the drift surfaces and the penetration point could be obtained simultaneously, the latter being defined by

$$\varphi^* = \int_0^{\lambda\tau} \dot{\varphi}\, dt \qquad (21)$$

where τ is the time of revolution.

In figs. 16 - 20 the calculated trajectories are compared with the measured ones. The calculations show that the small shear found has only a minor influence on the shape of the drift surfaces as the deviation from a circular cross section is hardly visible. The displacement of the centres of the drift surfaces belonging to one another is of the same order of magnitude as the calculated one. It should be noticed, however, that the circular cross section of the magnetic surfaces, which has been assumed for the calculations is obviously only a very crude approximation of the surfaces found in the experiment.

Conclusions

The measurements allow the conclusion that proper magnetic surfaces exist in W Ib with a high degree of probability. The deviation of the drift surfaces from a circular cross section also in the straight sections seems to be caused by the imperfect work of the circularizers and, perhaps, by the presence of the current leads.

For the evaluation of experiments on plasma confinement values of the rotational transform have to be used which are smaller by a factor of 0.88 than the values used earlier. The modest shear found is just on the limit where it could become effective for the stabilization of drift waves. The elliptical cross section of the magnetic surfaces requires some correction for the effective plasma volume and for the flux of plasma to a circular particle detector.

References

[1] E.Berkl
D.Eckhartt
G.von Gierke
G.Grieger
Phys.Rev.Lett. 17, 906 (1966)

[2] AEC Research and Development Report: The proposed model C stellarator facility

Figure Captions

Fig. 1 Schematic drawing of the stellarator W Ib

Fig. 2 Current distribution in the helical windings

Fig. 3 Influence of the correction fields on the displacement of the electron beam after one revolution and after correction for the torus drift

Fig. 4 Sequences observed, if $\iota \approx \frac{m}{n}$

Fig. 5 Nested particle surfaces. Case A. North side. $\approx 0.5\ \Pi$

Fig. 6 Surfaces on North-side, Case A $\iota \approx 0.500\ \Pi$

Fig. 7 Surfaces on North-side, Case A $\iota \approx 0.500\ \Pi$

Fig. 8 Surfaces on North-side, Case A $\iota \approx 0.500\ \Pi$

Fig. 9 Surfaces on North-side, Case B $\iota \approx 0.278\ \Pi$

Fig. 10 Surfaces on North-side, Case B $\iota \approx 0.278\ \Pi$

Fig. 11 Surfaces on North-side, Case B $\iota \approx 0.278\ \Pi$

Fig. 13 Surfaces on North-side, Case B $\iota \approx 0.278\ \Pi$

Fig. 14 Surfaces on North-side, Case C $\iota \approx 0.130\ \Pi$

Fig. 15 Surfaces on North-side, Case C $\iota \approx 0.130\ \Pi$

Fig. 16a Surfaces on South-side, Case A $\iota \approx 0.500\ \Pi$

Fig. 16b Surfaces on South-side, Case A numerically calculated surfaces $\iota = 0.500\ \Pi$

Fig. 17a Surfaces on South-side, Case B $\iota \approx 0.278\ \Pi$

Fig. 17b Surfaces on South-side, Case B numerically calculated surfaces $\iota = 0.278\ \Pi$

Fig. 18a Surfaces on South-side, Case B $\iota \approx 0.278\ \Pi$

Fig. 18b Surfaces on South-side, Case B numerically calculated surfaces $\iota = 0.278\ \Pi$

Fig. 19a Surfaces on South-side, Case B $\iota \approx 0.278\ \Pi$

Fig. 19b Surfaces on South-side, Case B numerically calculated surfaces $\iota = 0.278\ \Pi$

Fig. 20a Surfaces on South-side, Case C $\iota \approx 0.130\ \Pi$

Fig. 20b Surfaces on South-side, Case C numerically calculated surfaces $\iota = 0.130\ \Pi$

Fig. 21 vs. $\sqrt{ab}$

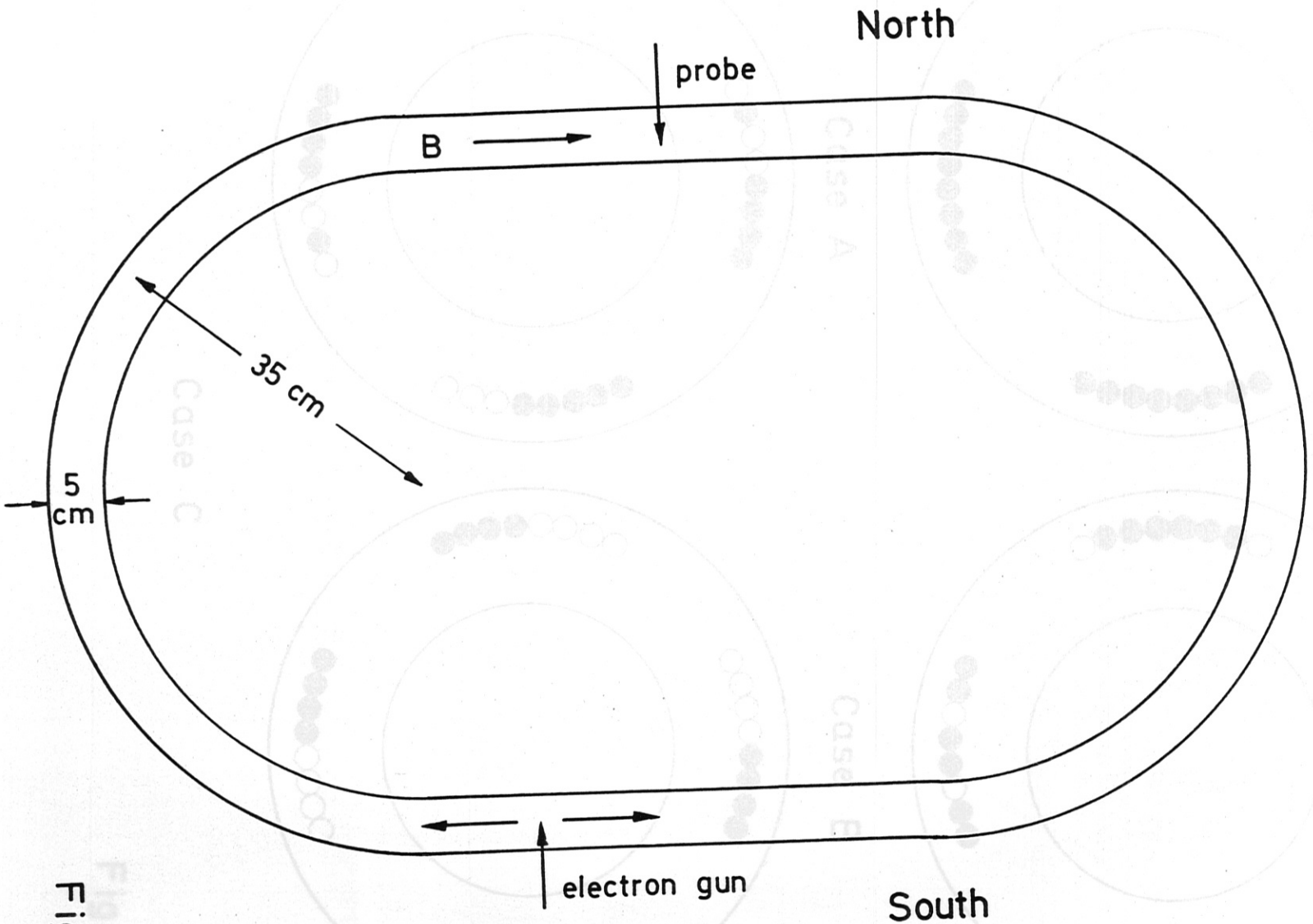

Fig. 1

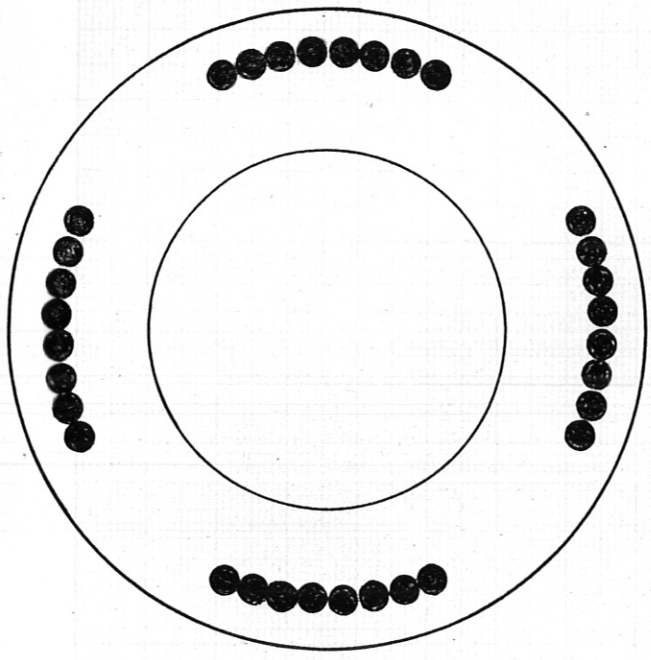

Case A

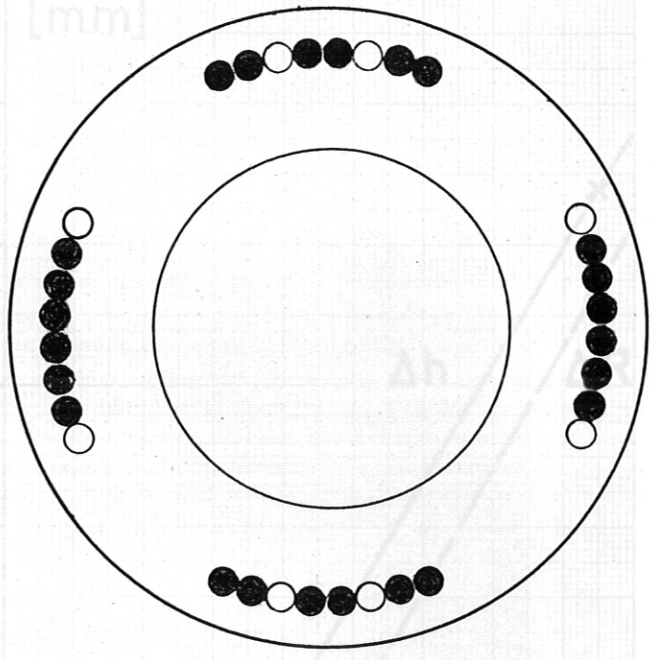

Case B

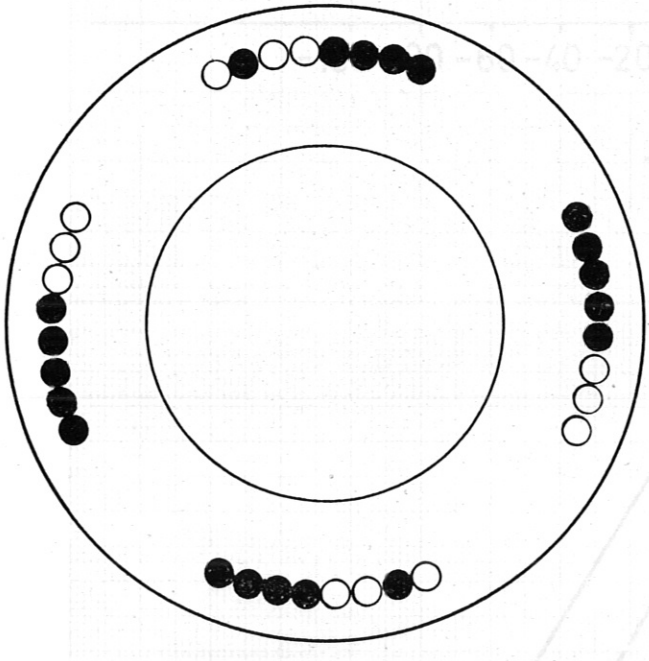

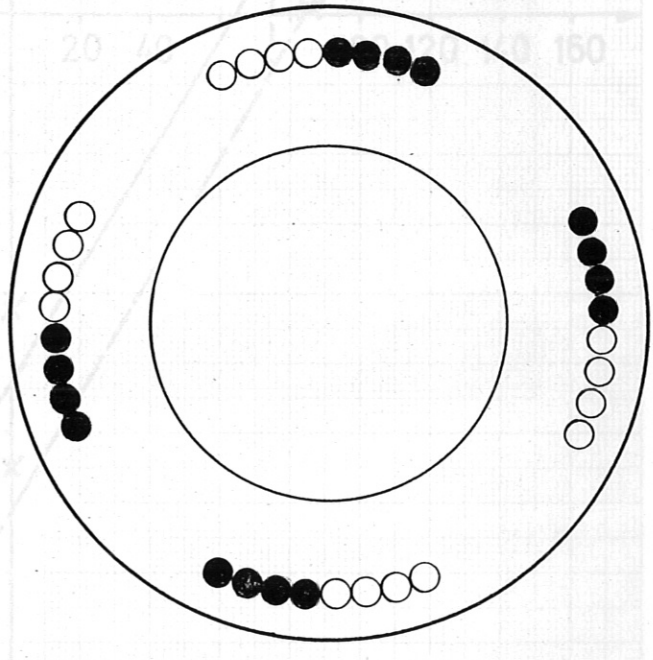

Case C

Fig. 2

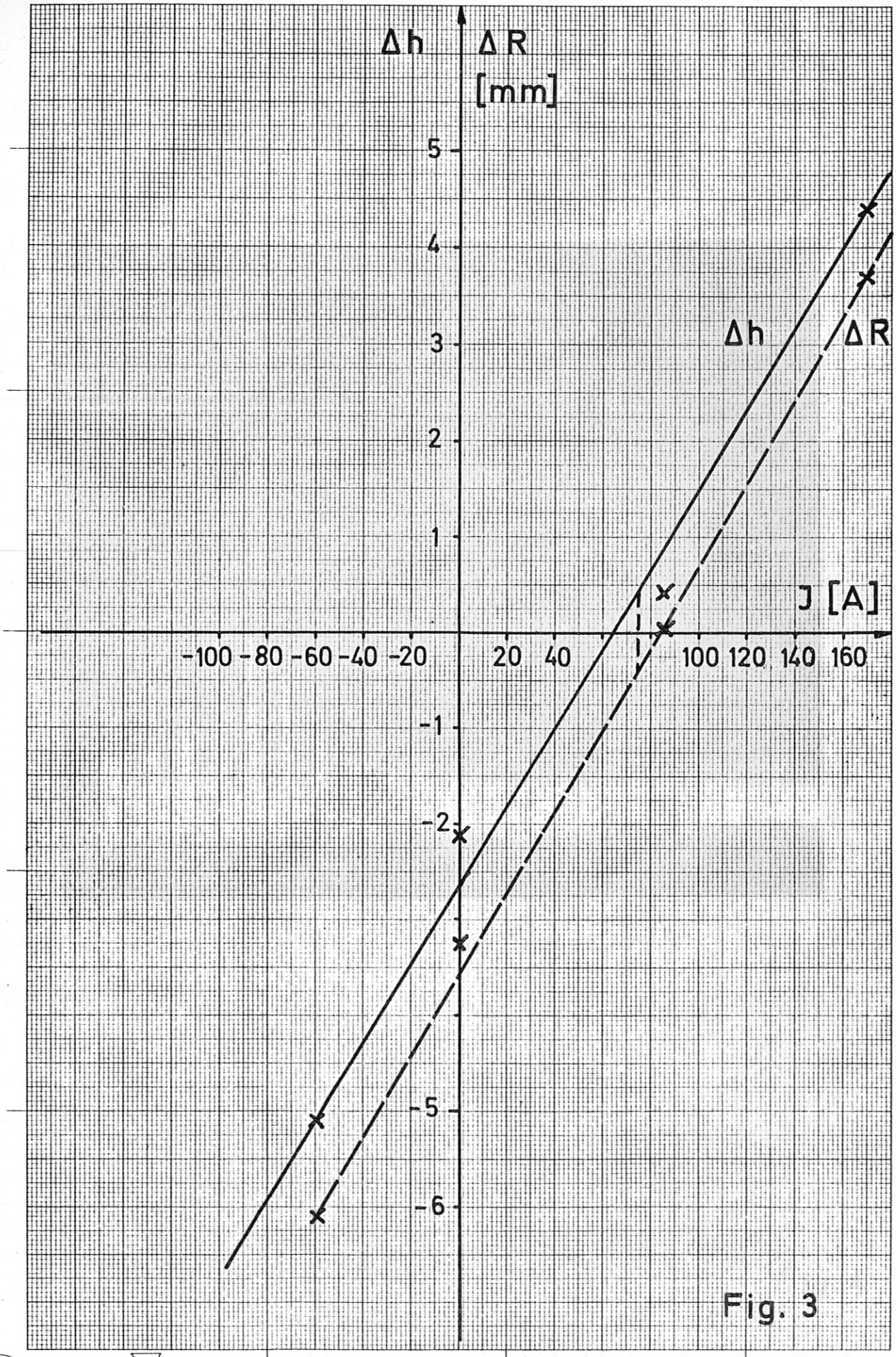

Fig. 3

15. 11. 67
10001

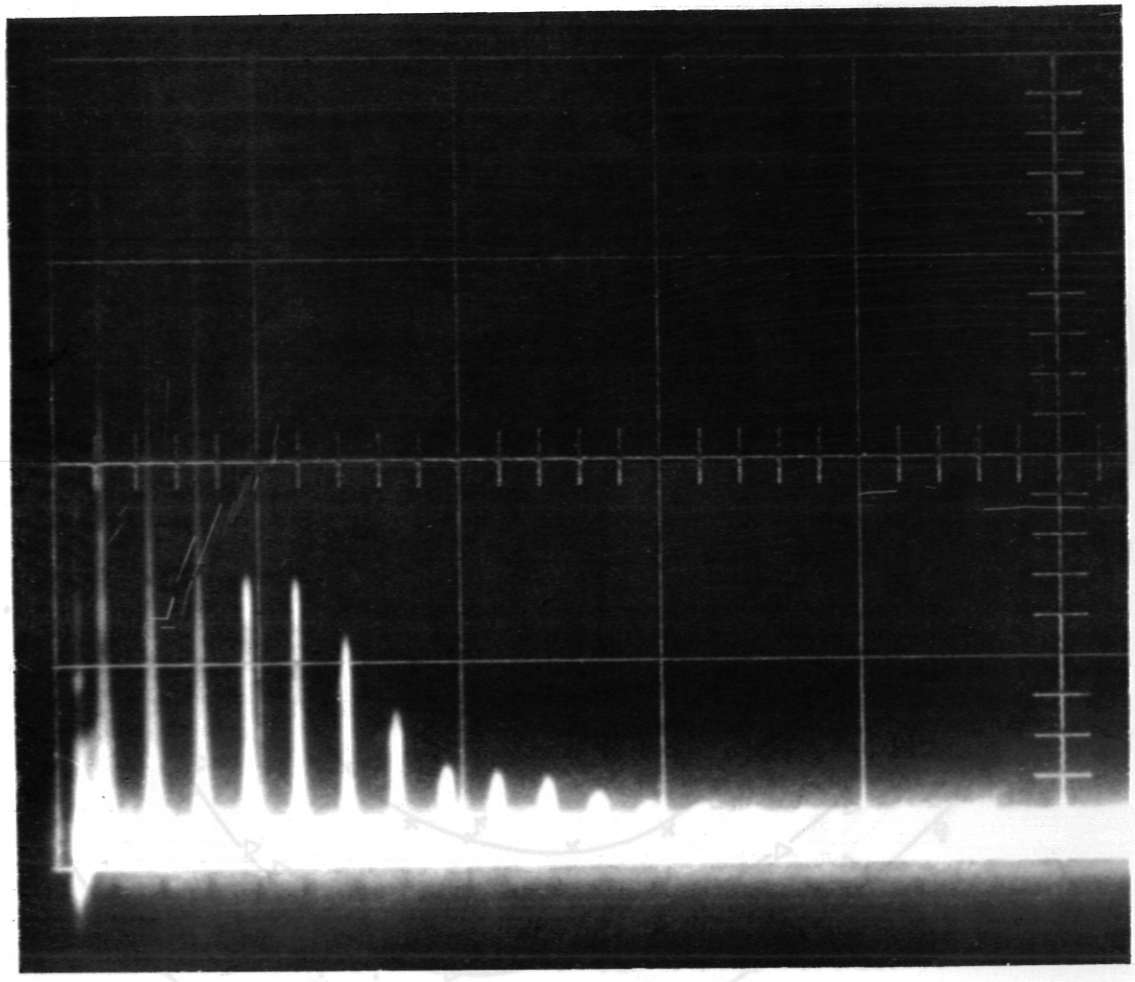

Fig. 4

20. 12. 67
10004

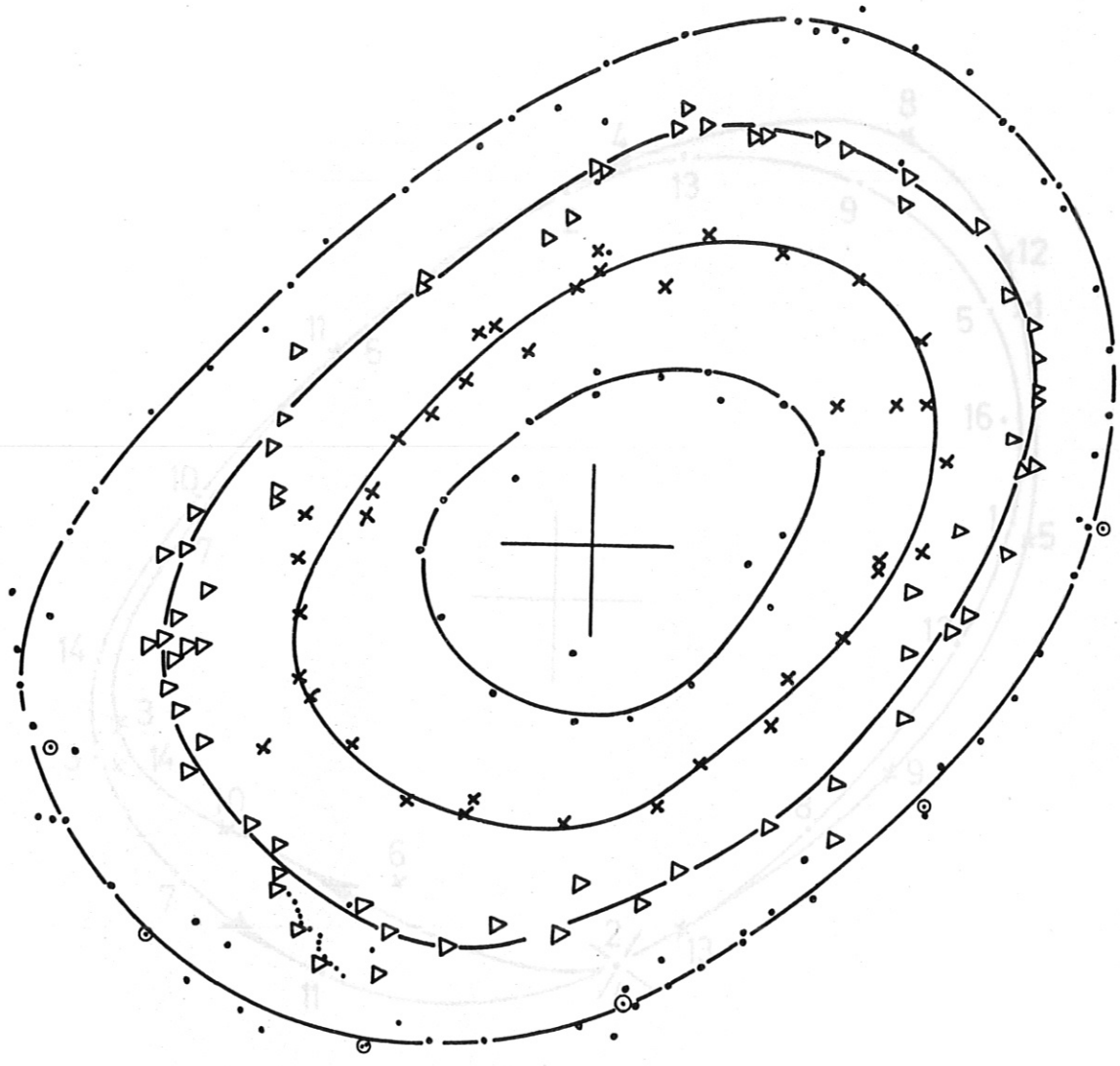

North, Case A

Fig. 5

23.1.68
10006

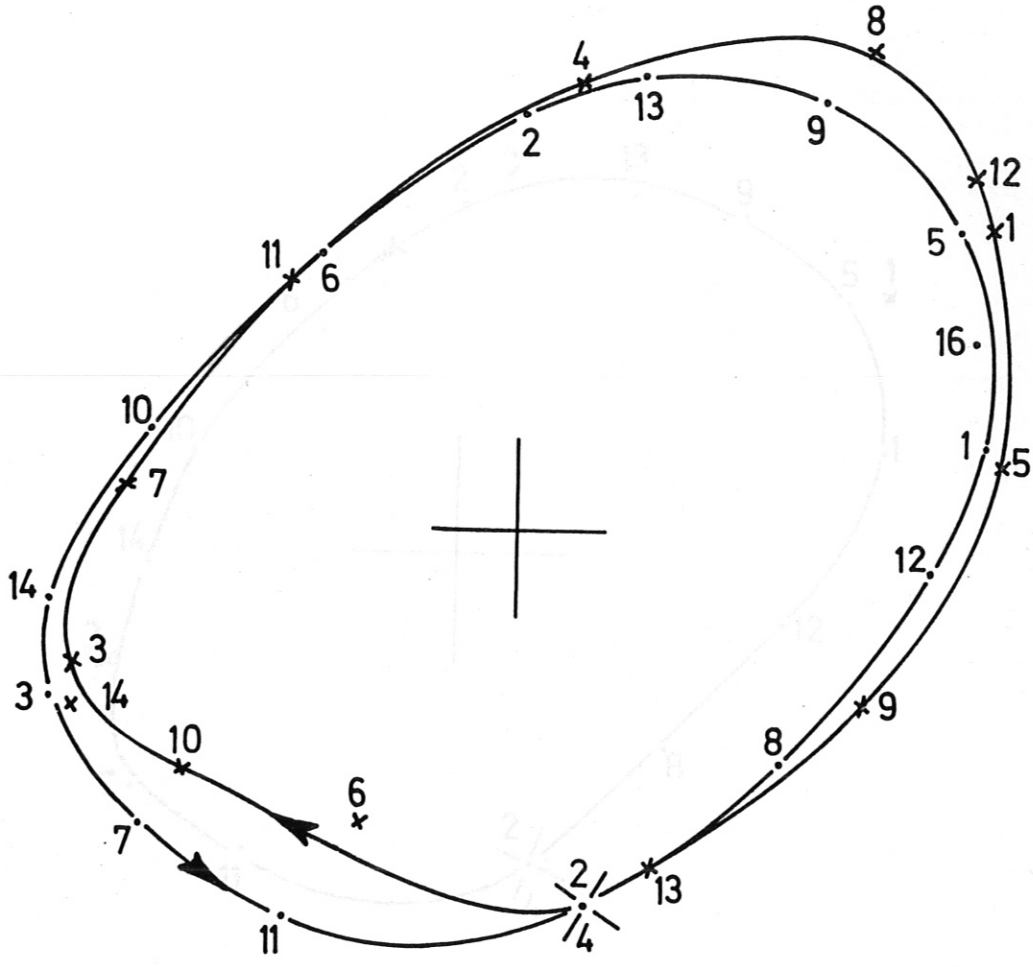

North, Case A

Fig. 6

23.1.68
10007

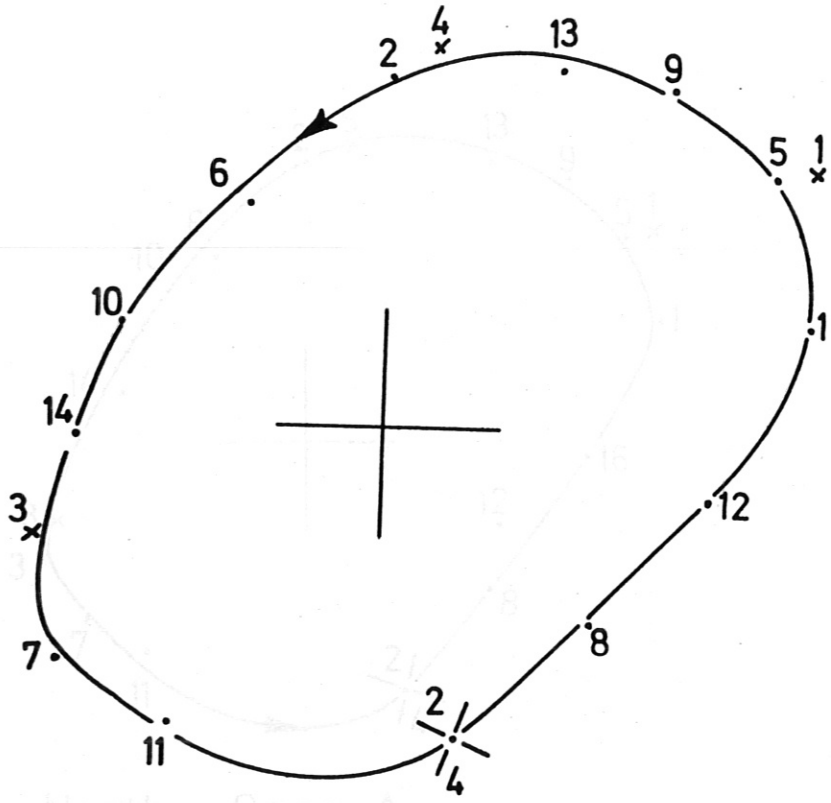

North, Case A

Fig. 7

23.1.68
10009

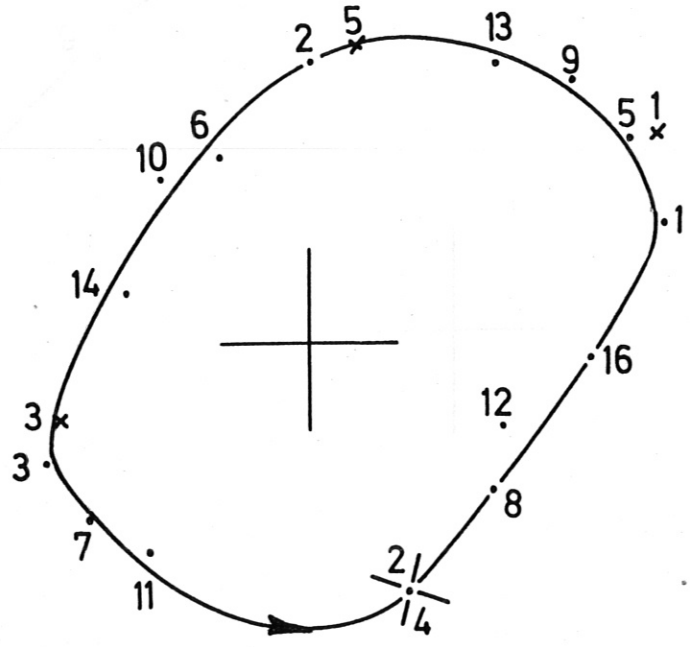

North, Case A

Fig. 8

8.1.68
10002

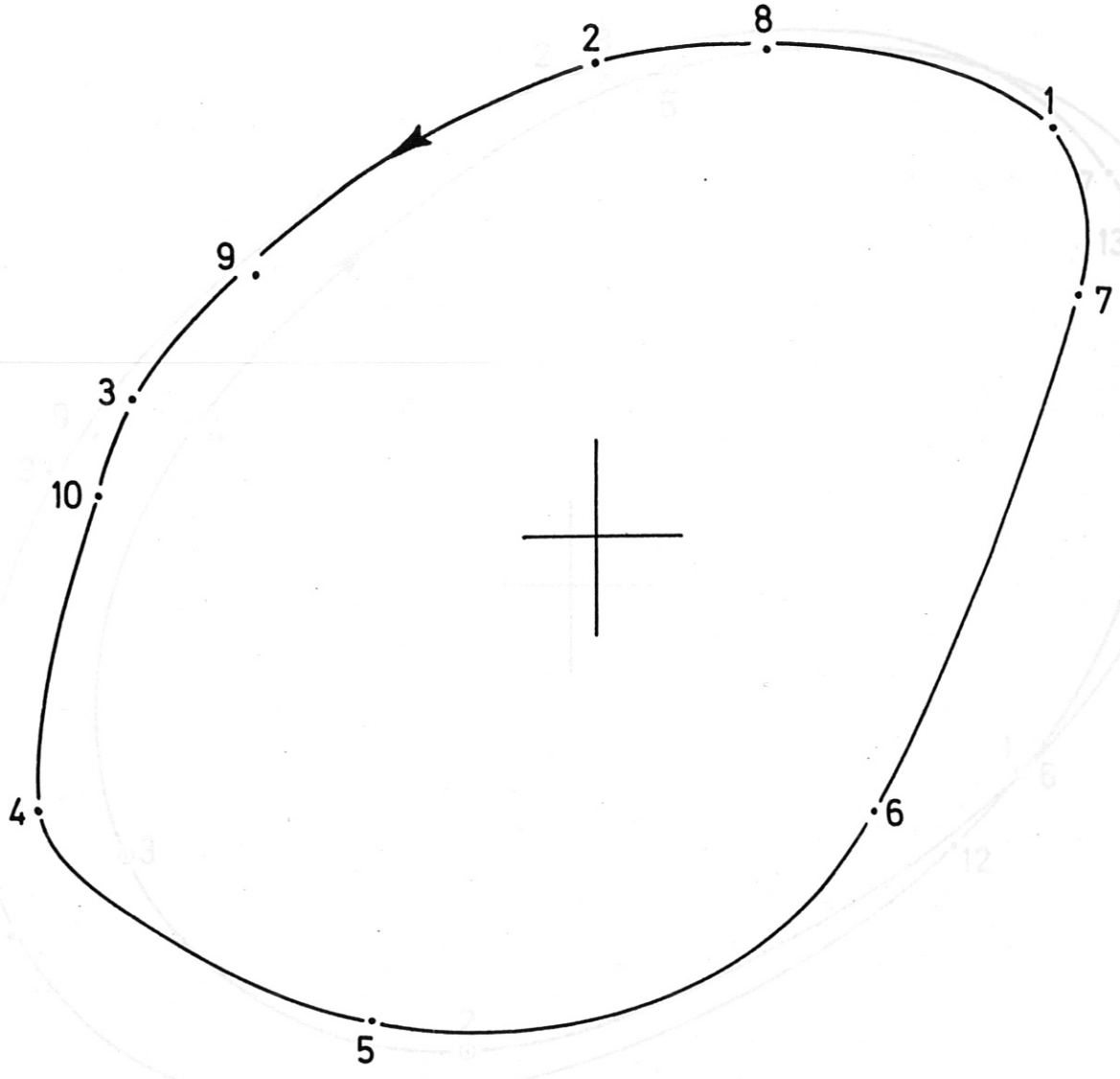

North, Case B

Fig. 9

12.1.68
10004

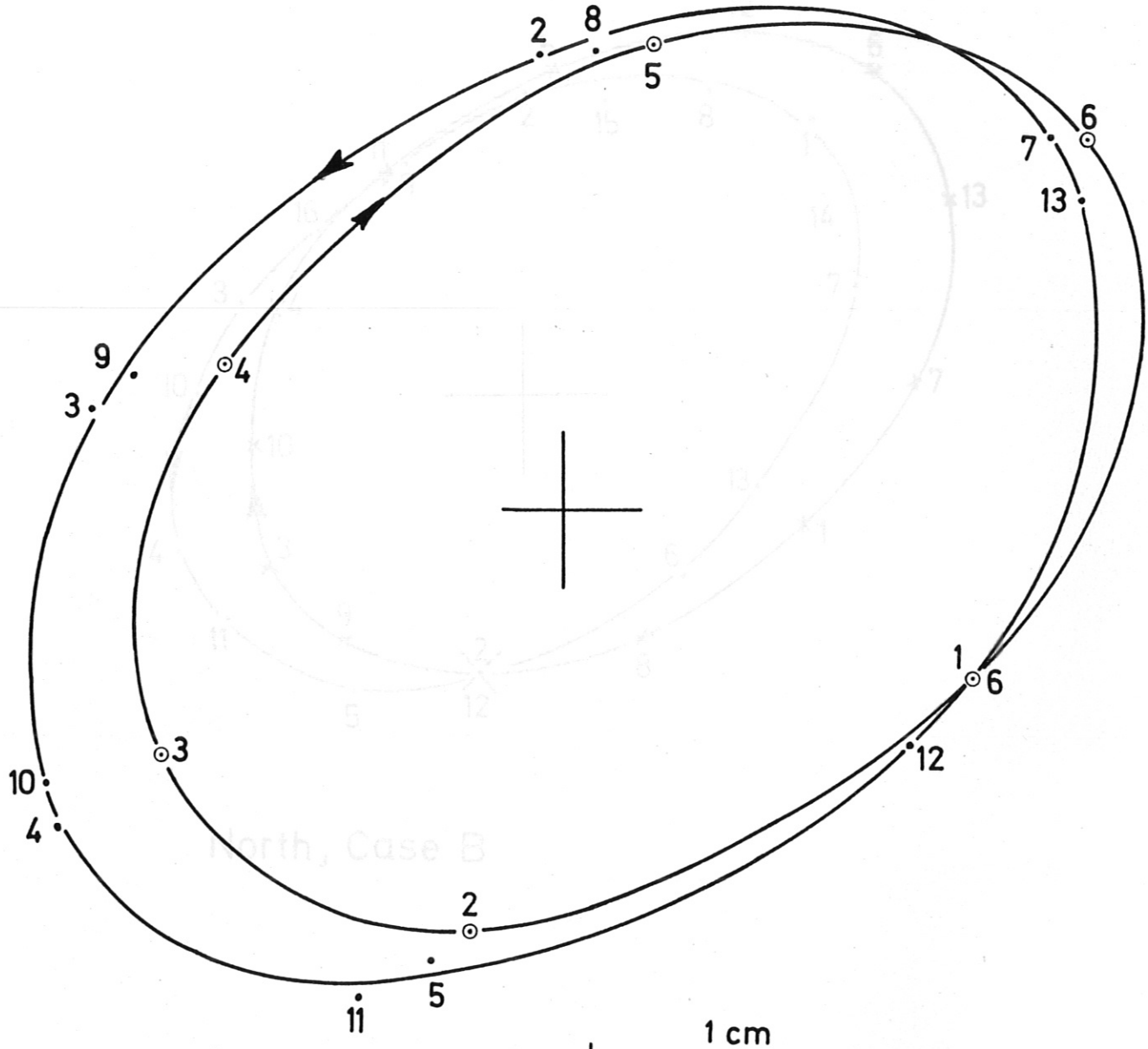

North, Case B

Fig. 10

23.1. 68
10002

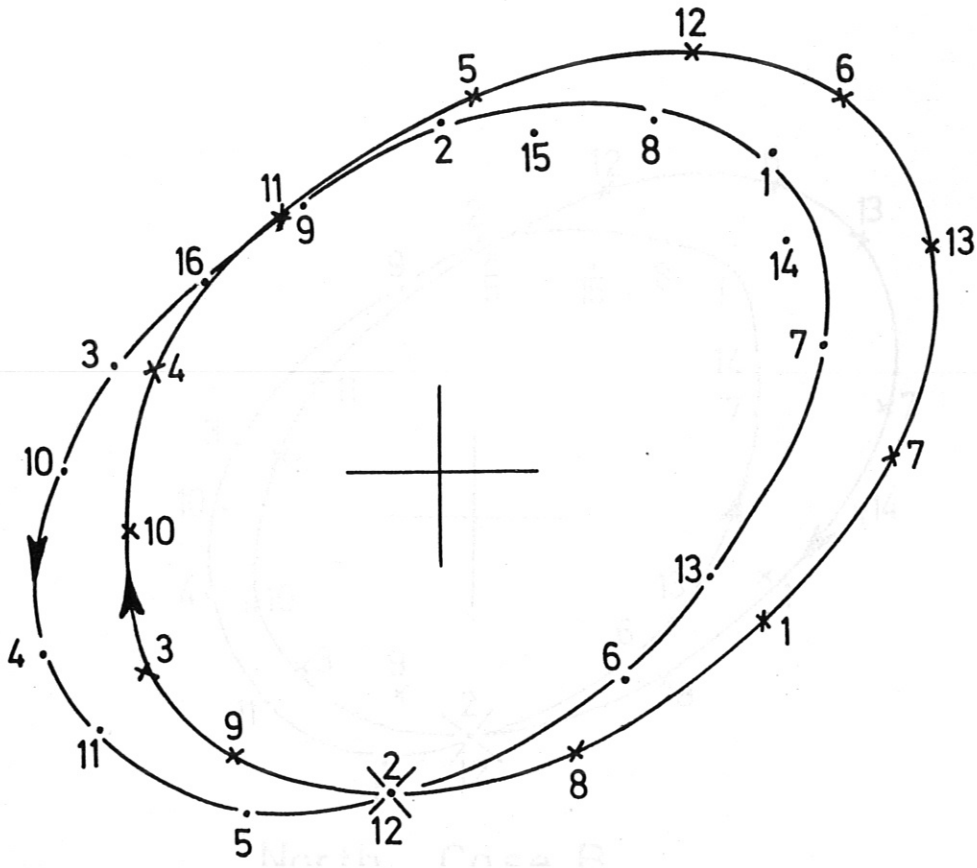

North, Case B

Fig. 11

23.1.68
10003

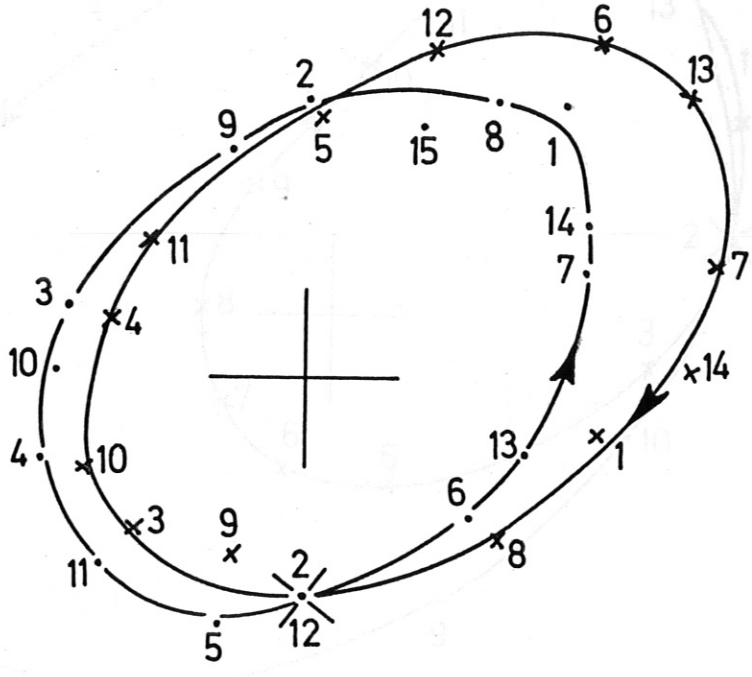

North, Case B

Fig. 13

29. 1. 68
10003

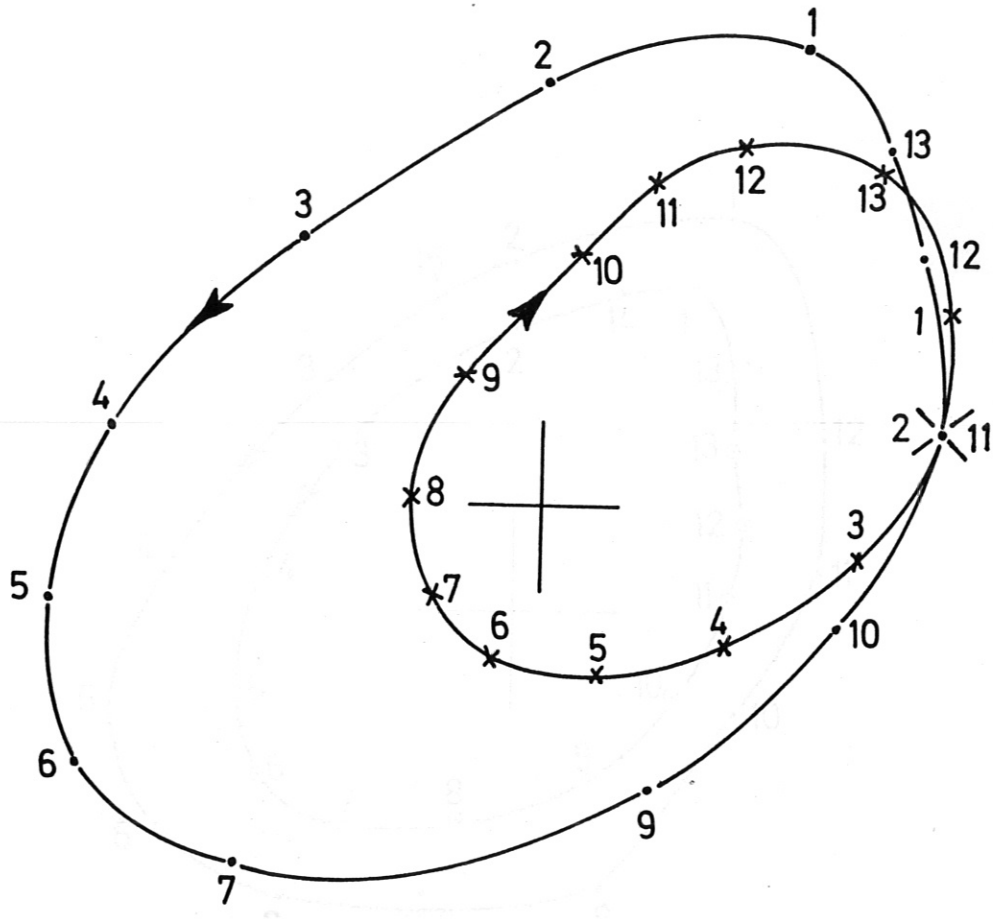

North, Case C

Fig. 14

29.1.68
10004

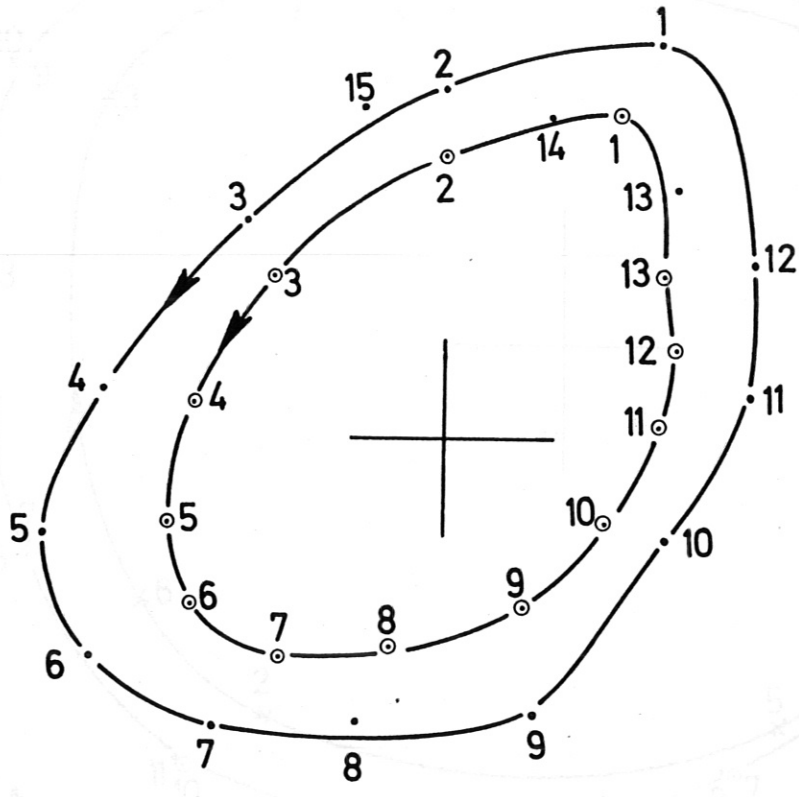

North, Case C

Fig. 15

31. 1. 68
10006

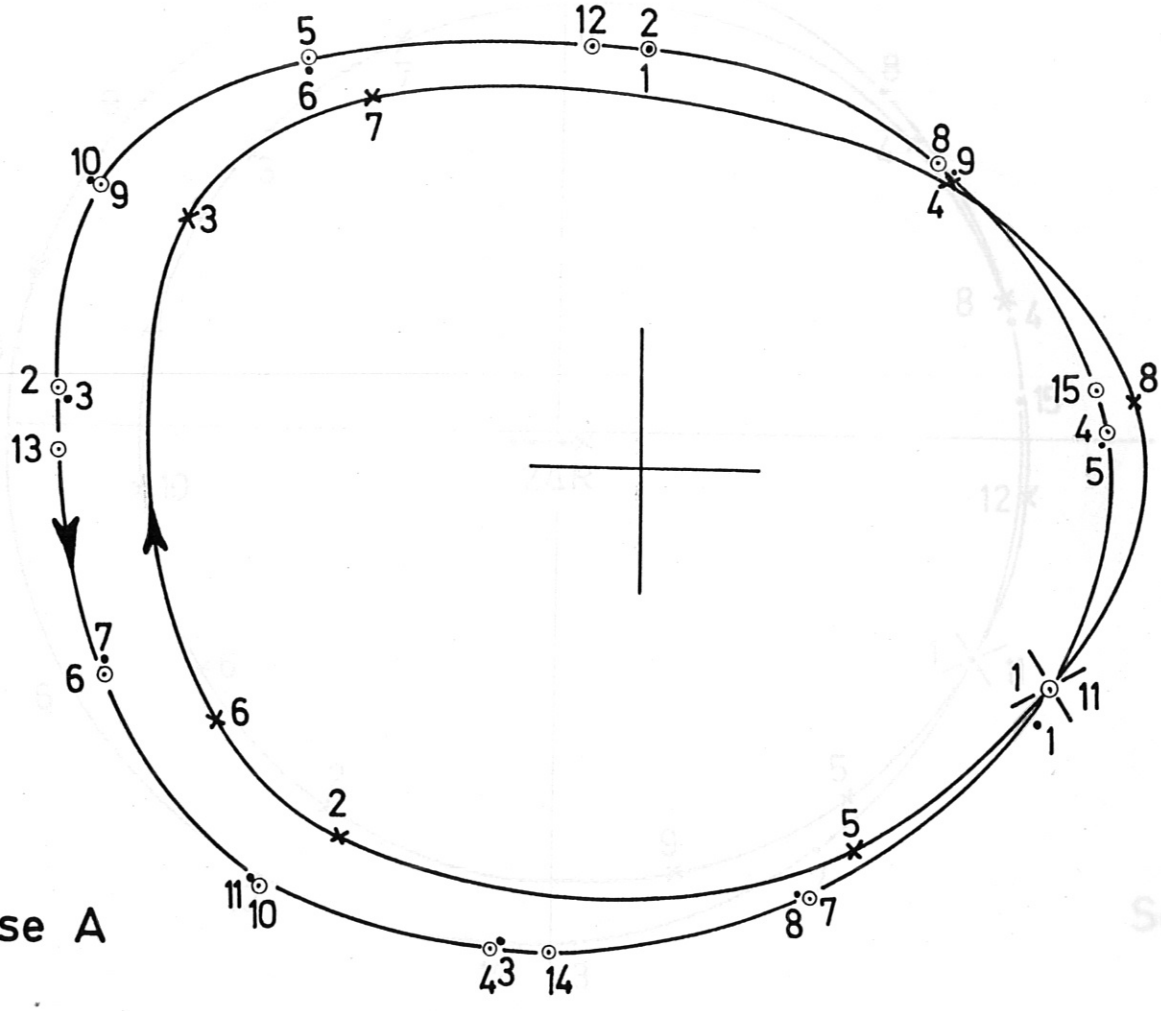

Case A

Fig. 16a

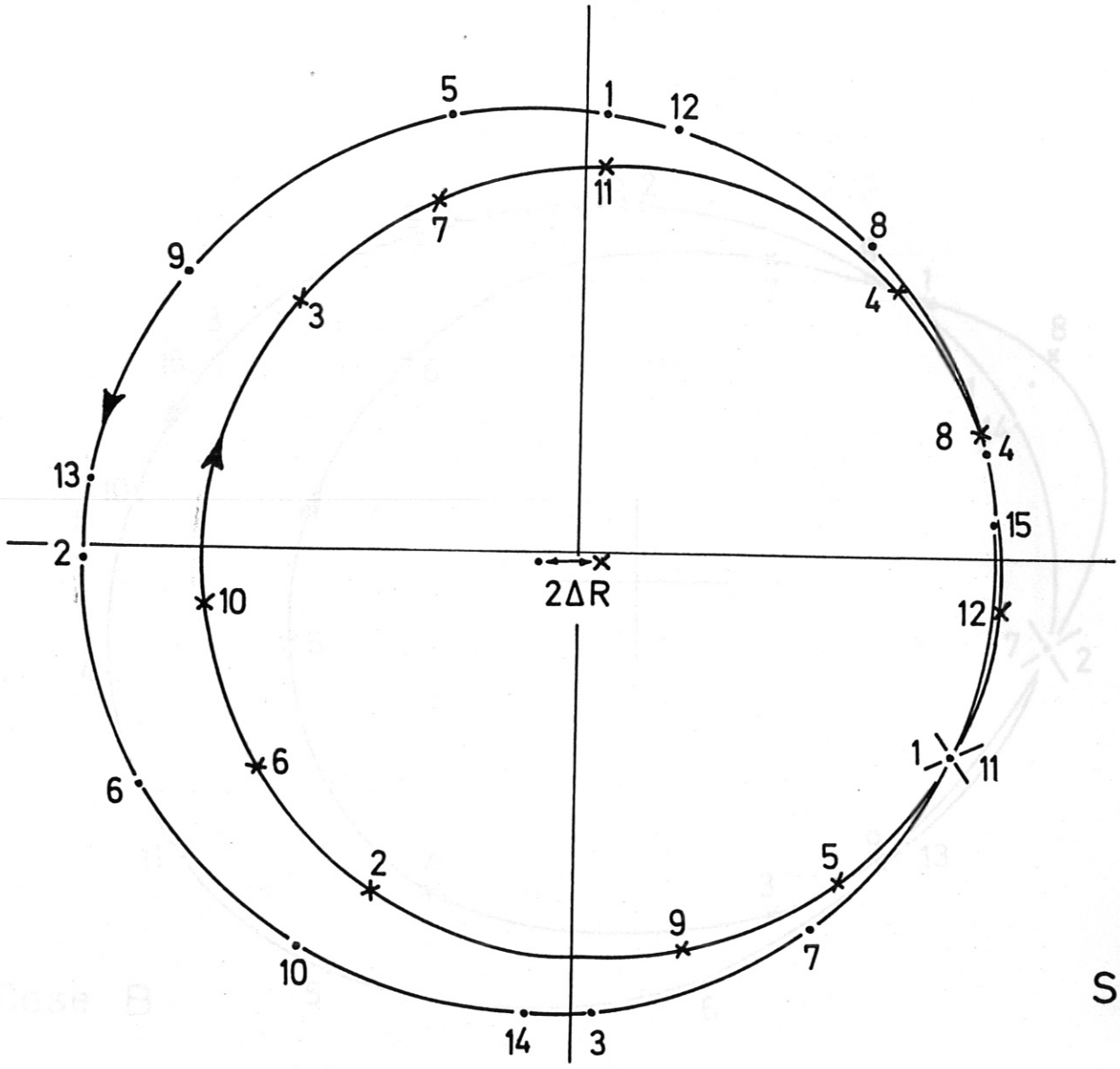

South,

Fig. 16b

30.1.68
10004

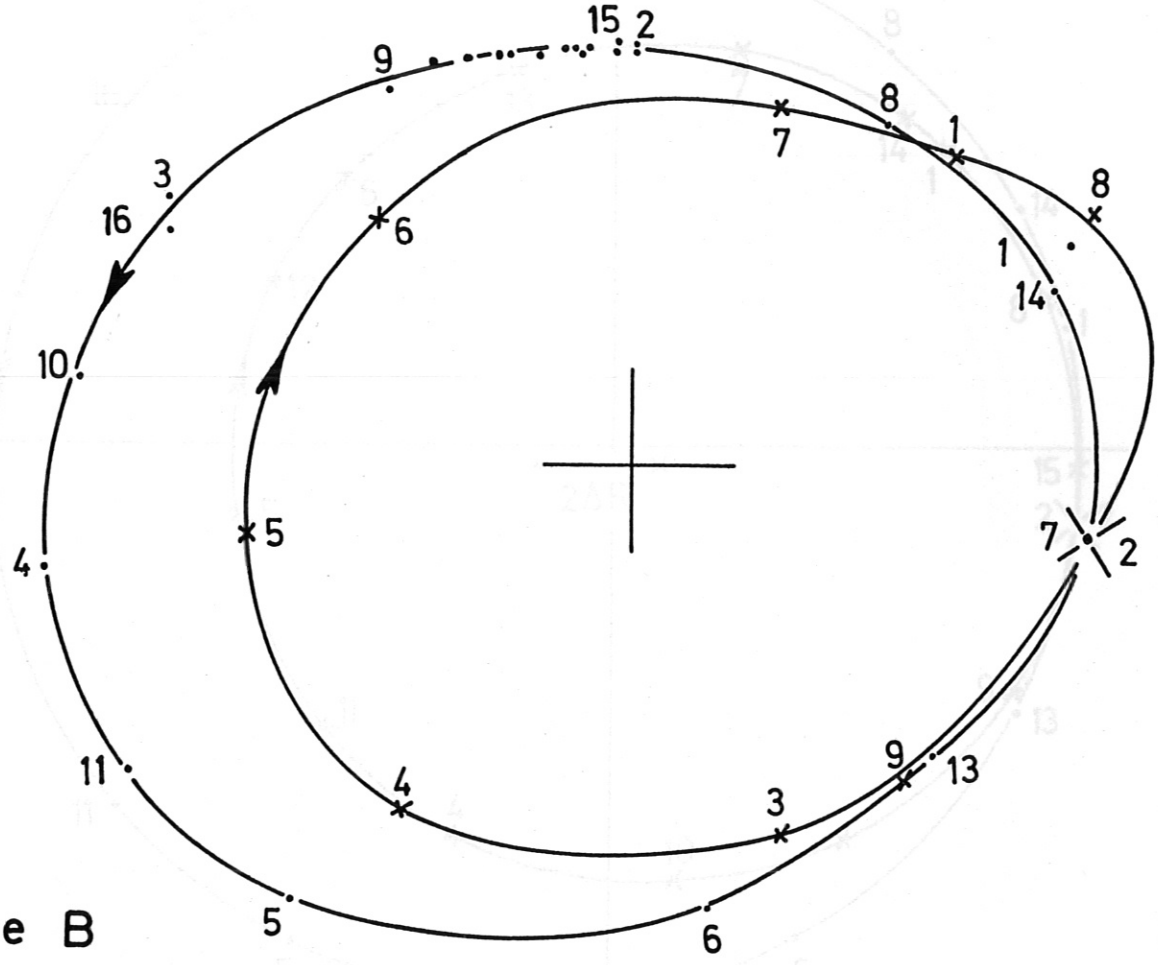

Case B

Fig. 17a

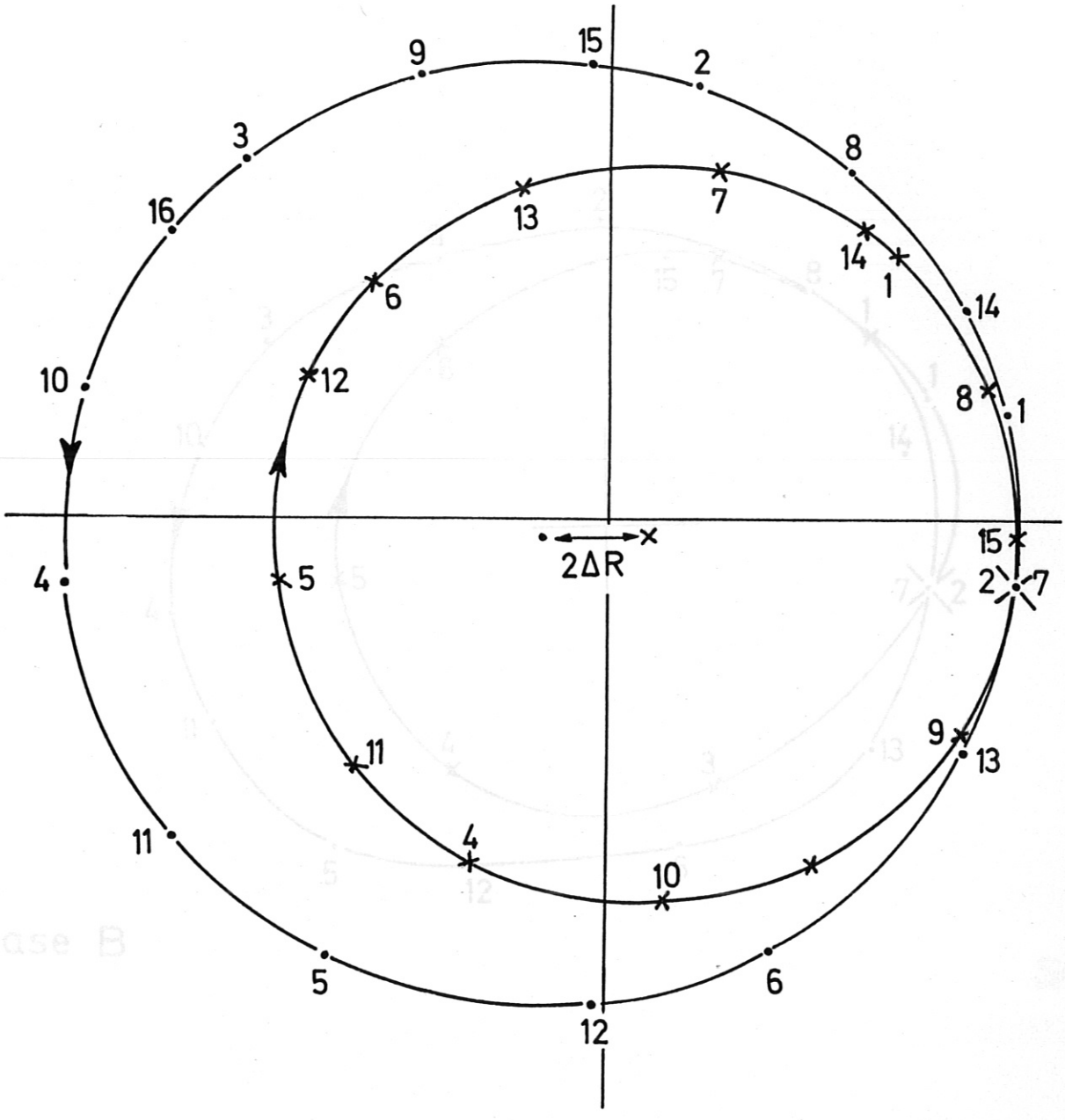

South,

Fig. 17 b

31. 1. 68
10002

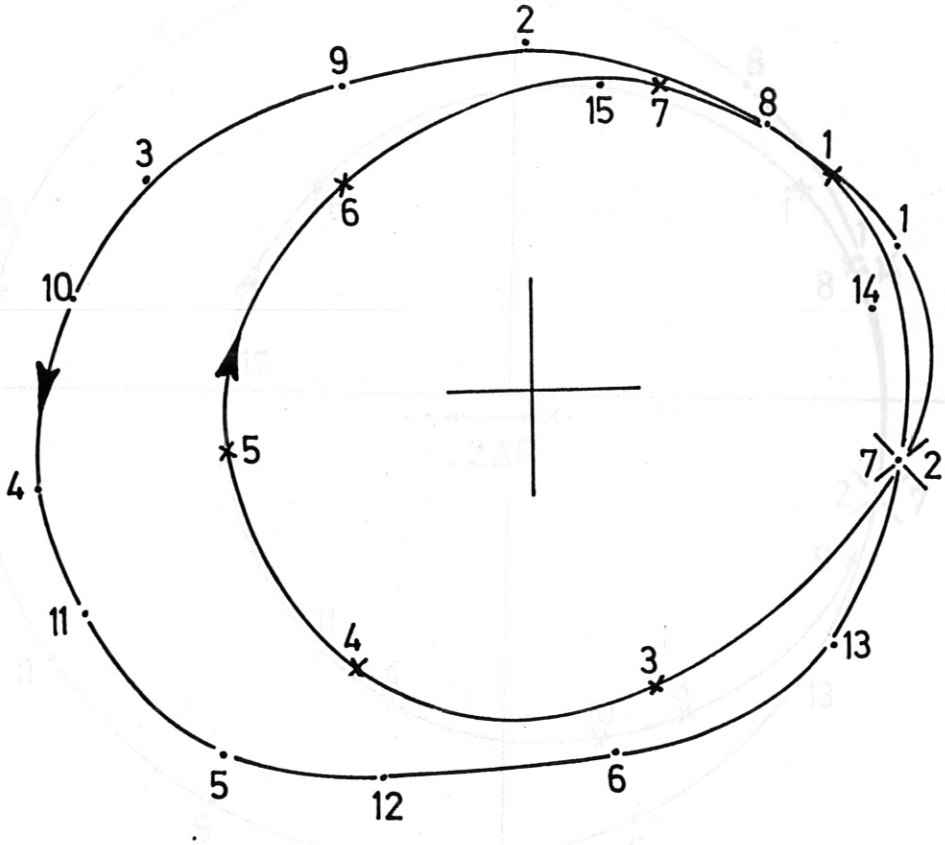

Case B

Fig. 18 a

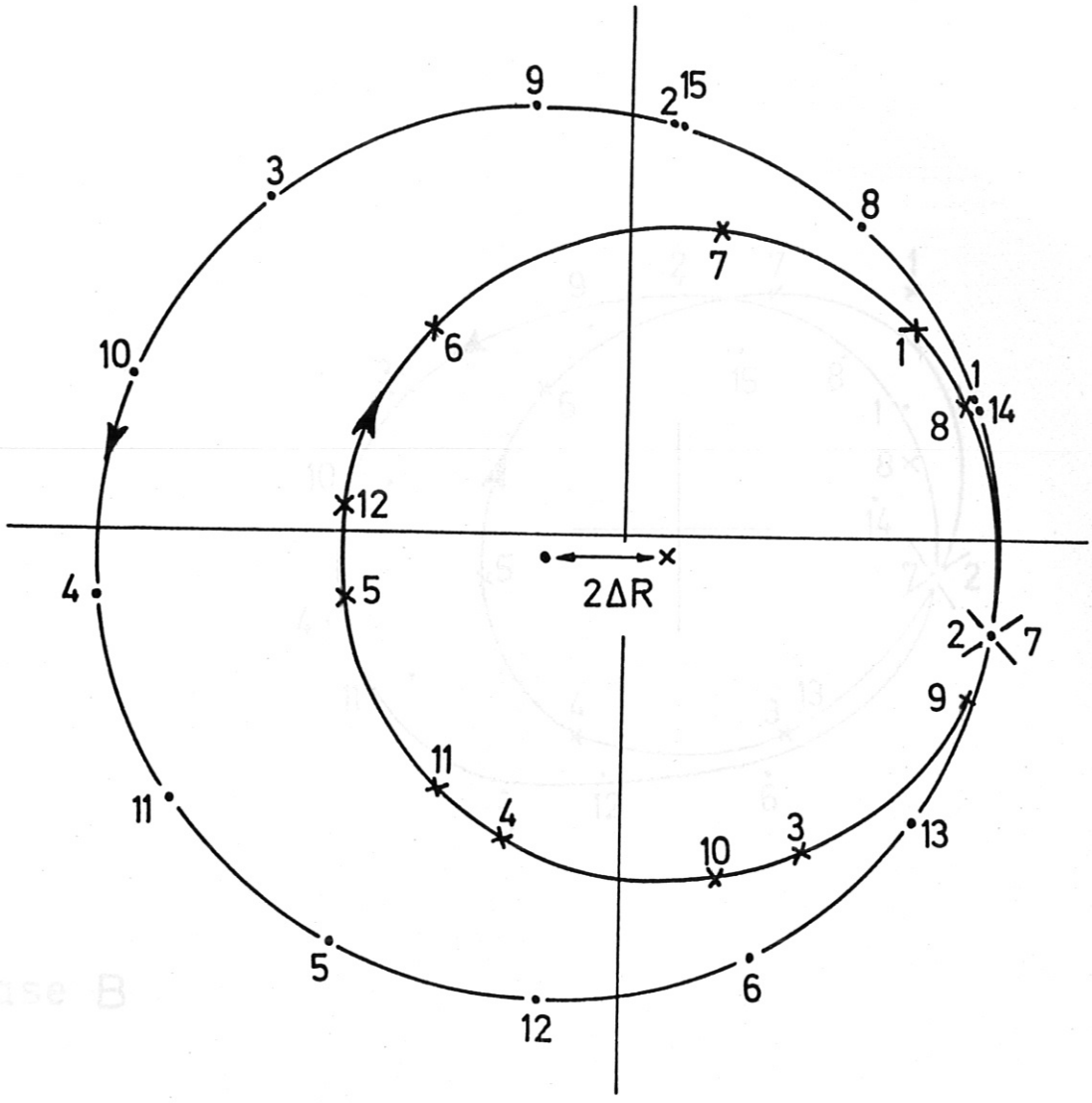

South,

Fig. 18 b

31. 1. 68
10004

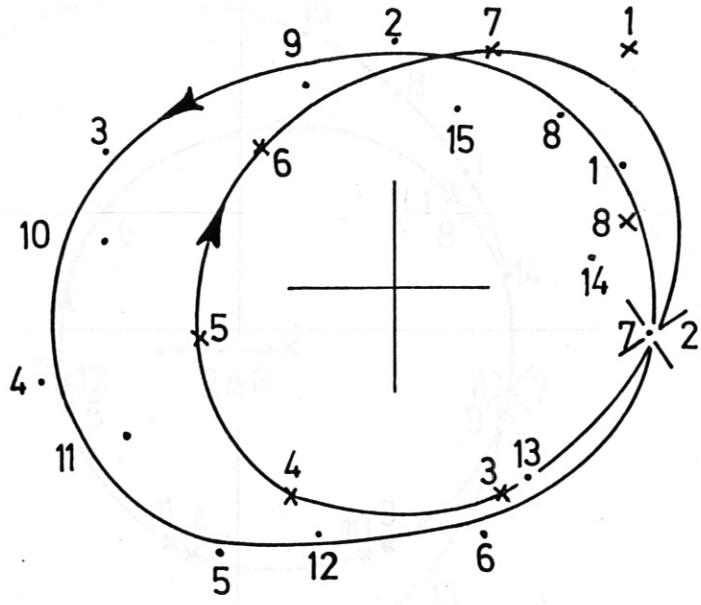

Case B

Fig. 19a

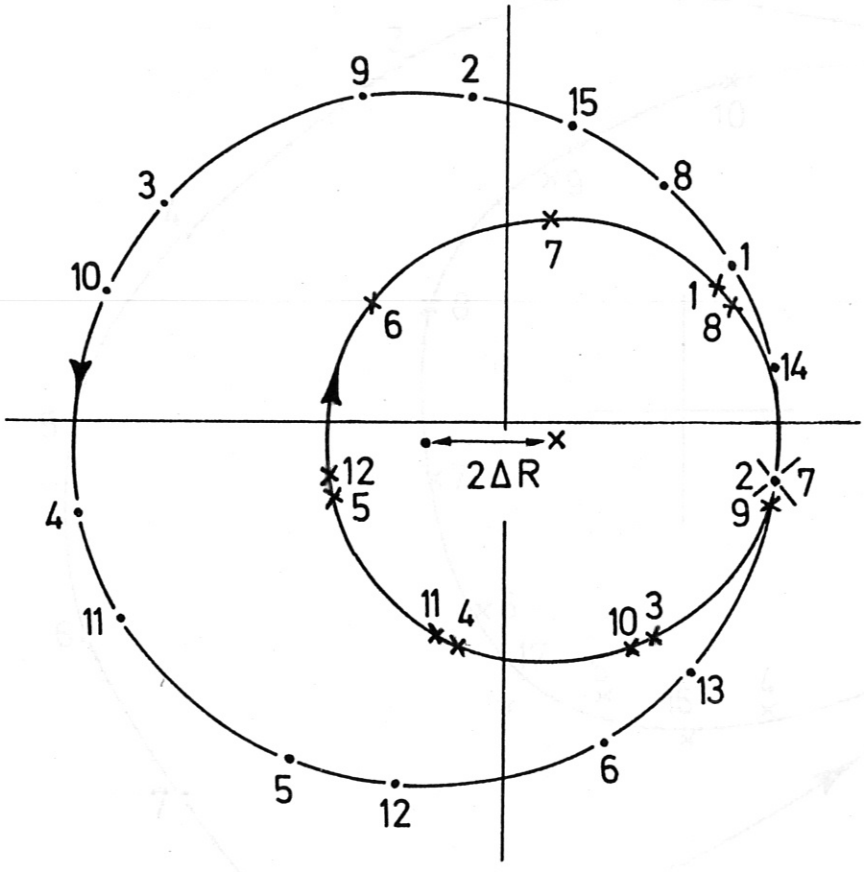

South,

Fig. 19 b

30.1.68
10002

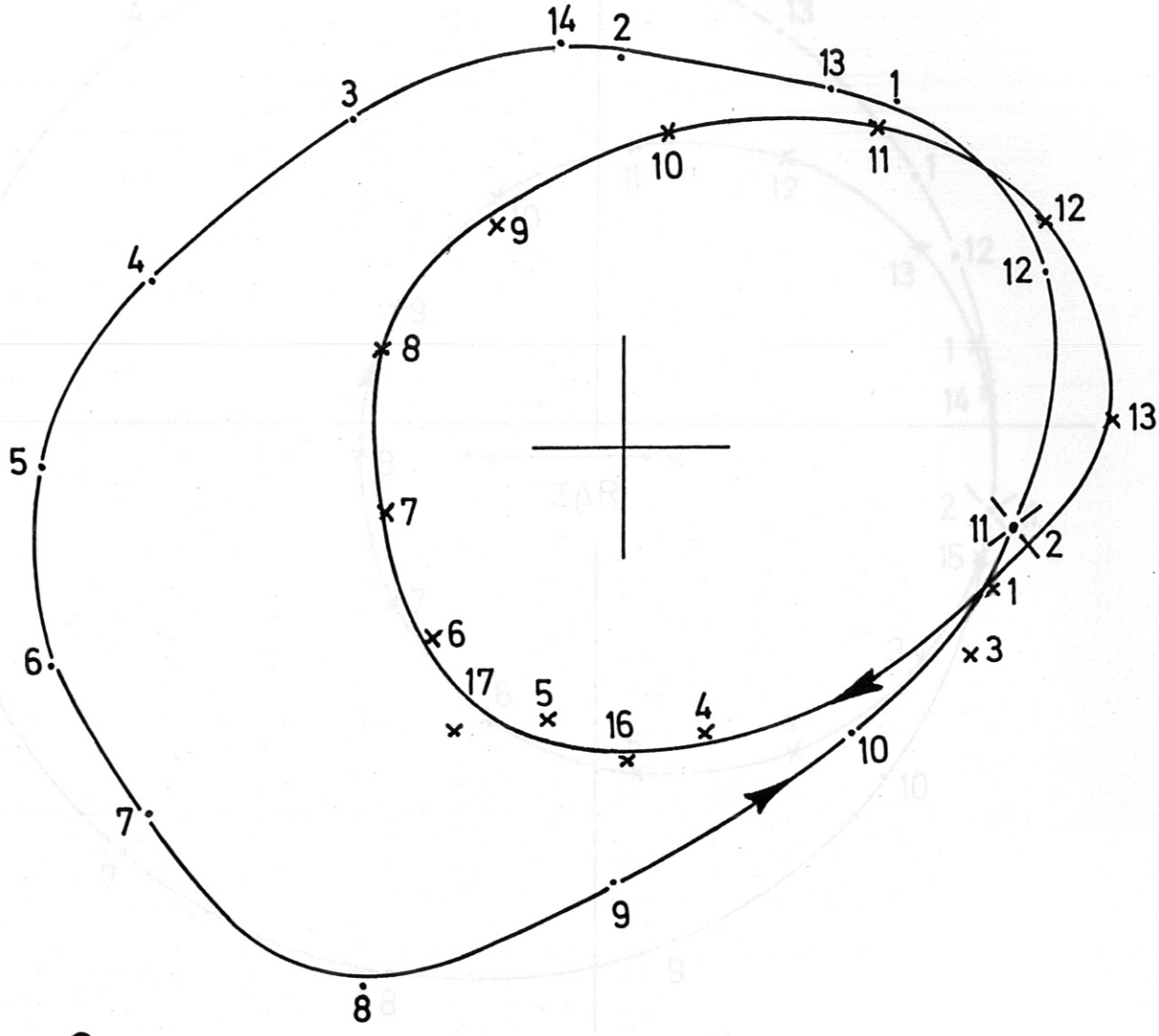

Case C

Fig. 20a

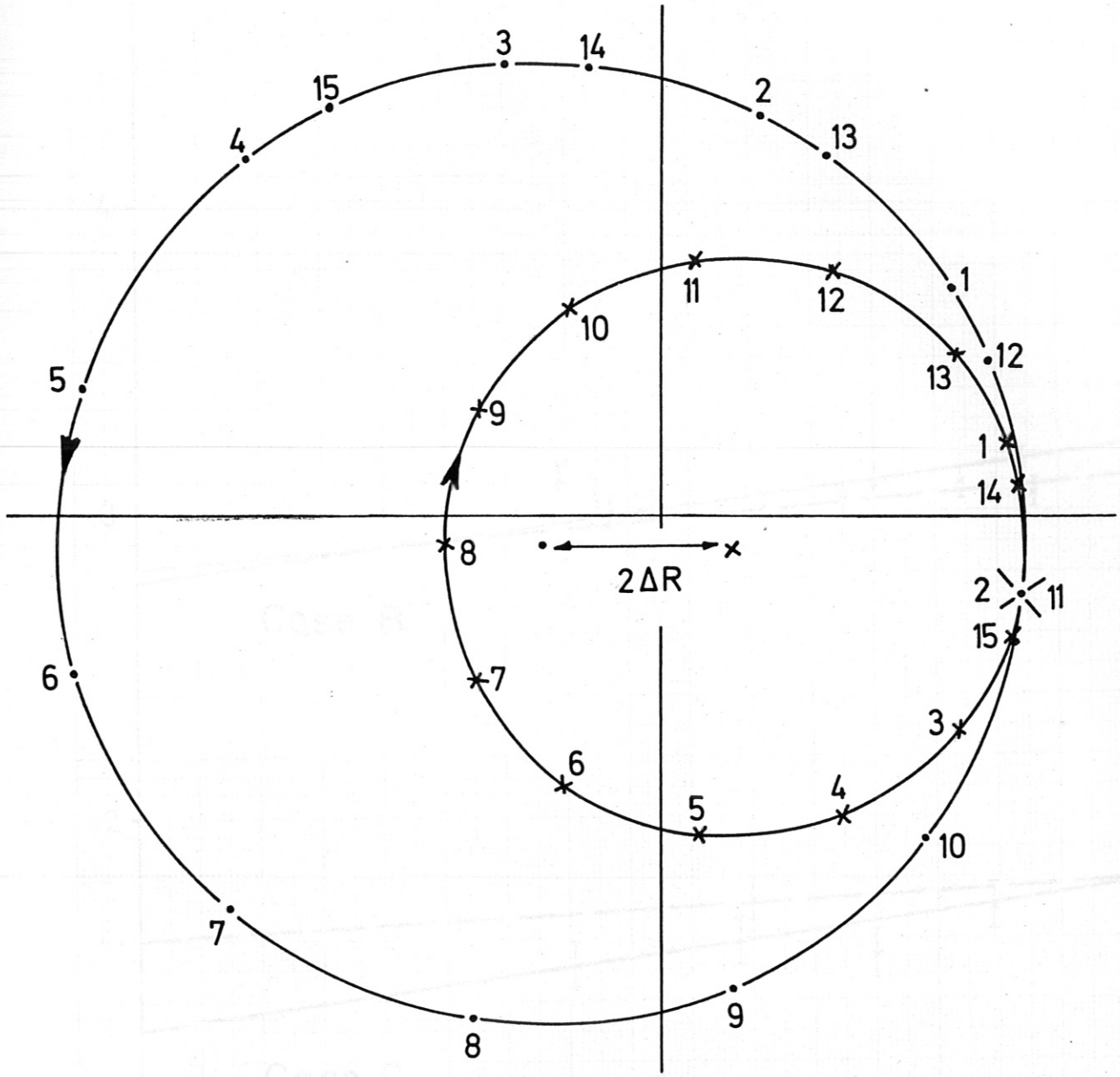

South,

Fig. 20 b

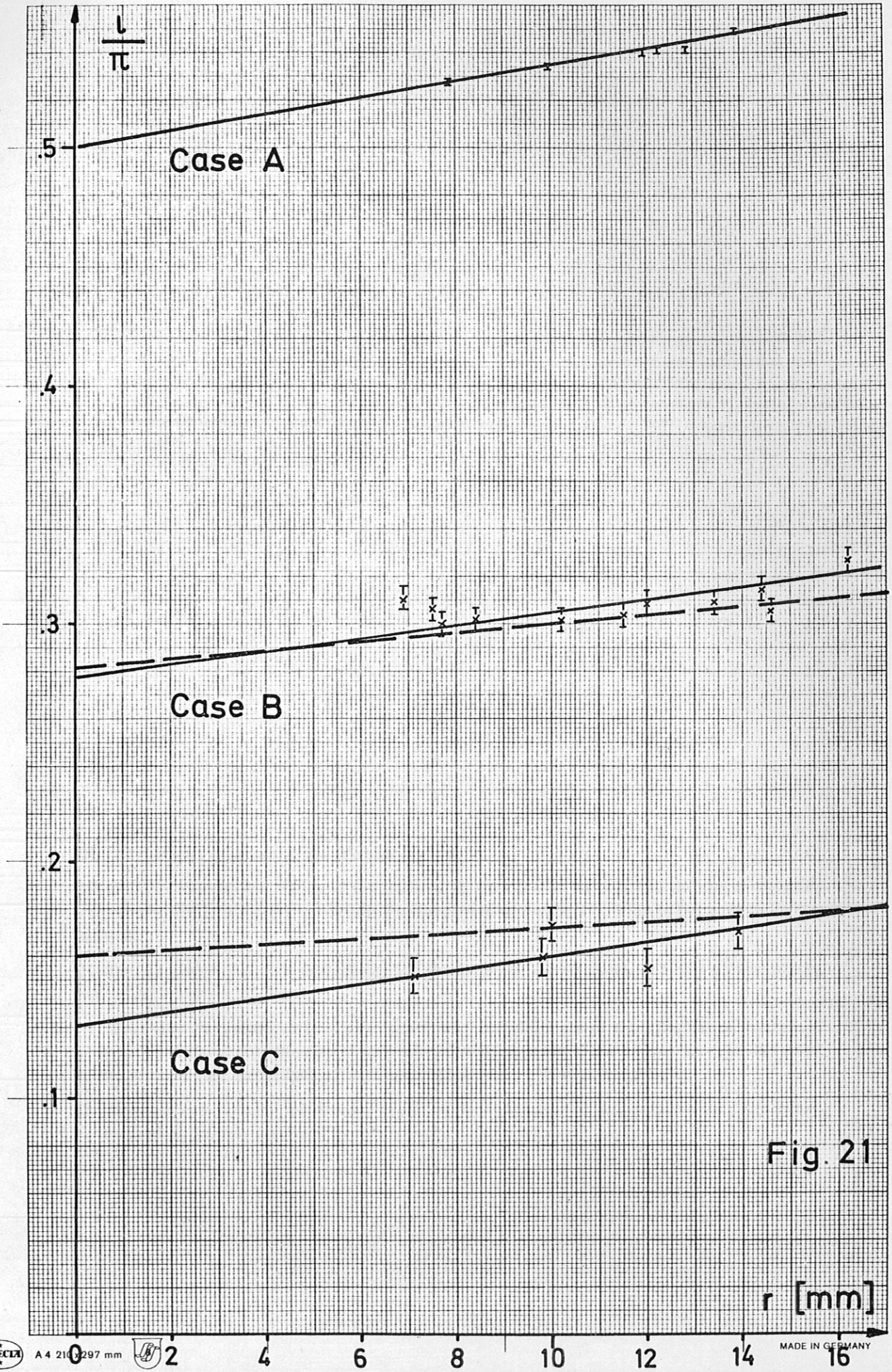

Fig. 21